Electrochimica Acta 54 (2009) 4397–4402

Contents lists available at ScienceDirect

Electrochimica Acta

journal homepage: www.elsevier.com/locate/electacta

Copper extraction from copper ore by electro-reduction in molten $CaCl_2$–NaCl

Xinlei Ge[a,b,*], Xidong Wang[c], Seshadri Seetharaman[a]

[a] Department of Materials Science and Engineering, Royal Institute of Technology, SE 100 44, Stockholm, Sweden
[b] Department of Physical Chemistry, University of Science and Technology, Beijing, 100083, China
[c] College of Engineering, Peking University, Beijing, 100871, China

ARTICLE INFO

Article history:
Received 24 October 2008
Received in revised form 7 March 2009
Accepted 9 March 2009
Available online 20 March 2009

Keywords:
Copper extraction
Electro-reduction
Molten salts
Green process
SO_2 emission

ABSTRACT

Sintered solid porous pellets of copper sulfide (Cu_2S) and Cu_2S/FeS were electrolysed at a cell voltage of 2.2–2.8 V to elemental Cu, S and Cu, Fe, S, respectively in molten $CaCl_2$–NaCl at 800 °C under the protection of argon gas. The process parameters for optimal electrolysis are presented. The electrolysis products are characterized by microscopic techniques and XRD. The product characteristics are linked to the process parameters. The direct electrolysis of the sulfide to copper with the emission of elemental sulphur offers an attractive green process route for the treatment of copper ore.

1. Introduction

Over 90% of the world's primary copper on the earth's crust is present in the form of sulfide minerals, such as chalcocite (Cu_2S), chalcopyrite ($CuFeS_2$) and bornite (Cu_5FeS_4), which are always treated by pyrometallurgical processes [1]. Copper also occurs in the form of oxidic ores (carbonates, oxides, silicates, sulphates) to a much lesser extent. The latter can be treated by heap-leaching together with solvent extraction and electro-winning, or by bacteria-aided bioleaching. For sulfide ores, after concentration by froth flotation, the extraction of copper is carried out with the following three steps: (a) roasting, (b) matte smelting (in blast, reverberatory, electric or flash furnaces) and (c) converting to blister copper. These three steps can also be combined into a continuous process [1]. However, emission of SO_2, despite the cost-intensive modern techniques of SO_2-capture, is a difficult problem considering the increased environmental restrictions.

Thus, it is essential to find a method to capture most of the sulphur in a stable form, especially as elemental sulphur. In the past few years, a generic process [2–4] for producing metal and alloy by direct electrochemical reduction of corresponding metal compound or mixtures has attracted worldwide attention, because of its lower energy consumption and simple operation. Many efforts have been paid on the direct reduction of pure or mixed oxides [5–20]. However, very little work has so far been carried out in the electrolytic reduction of sulfides. Li et al. [21] had investigated the electrolysis of MoS_2. Chen and Fray [22] have examined the removal of S in liquid copper. The present work aims to demonstrate a potential of the electro-reduction route towards copper extraction from sulfide material aiming at capturing sulphur in the elemental form.

2. Experimental

2.1. Thermodynamic principles

Even though the electro-reduction principles have been presented in a number of earlier publications [5–20], a brief outline is given here in order to orient the readers to the context of this paper. The oxide or sulfide compact, wrapped by a metal gauze is used as a cathode in an electrolytic process using molten $CaCl_2$/$CaCl_2$–NaCl electrolyte in the temperature range of 700–1000 °C. Graphite is normally used as the anode. The oxide or sulfide gets reduced to the metallic state.

During the above process with respect to oxide materials, the use of graphite anodes leads inevitably to the carbon getting oxidized, leading to the emission of CO and CO_2. This, in turn, has negative environmental consequences. In addition, the consumption of graphite during the process has an adverse economic impact. On the other hand, use of inert materials would add a cost factor and has not been favoured in industrial practice. In the present case, sulphur would be released at the anode leading to the reaction between elemental sulphur and carbon forming carbon sulfides. It

* Corresponding author at: Department of Materials Science and Engineering, Royal Institute of Technology, Brinellvagen 23, SE 100 44, Stockholm, Sweden. Tel.: +46 08790 8326.
E-mail address: xinleige@yahoo.com.cn (X. Ge).

0013-4686/$ – see front matter.
doi:10.1016/j.electacta.2009.03.015

is imperative that these reactions are carefully controlled, since CS_2 is very harmful to fauna.

In this respect, the following reactions are considered:

$$C + S_2 = CS_2, \qquad \Delta G^\circ(1073\,K) = -18.23\,kJ, \tag{1}$$

$$C + 0.5S_2 = CS, \qquad \Delta G^\circ(1073\,K) = 118.59\,kJ, \tag{2}$$

The values of standard Gibbs free energy in this work were all calculated by Factsage Software [23–24], and the theoretical decomposition voltages of Cu_2S, Cu_2O and FeS shown in the following sections were estimated from their corresponding Gibbs energy values.

It can be seen that the formation of CS is not thermodynamically favoured. On the other hand, CS_2 formation is favourable, but Gibbs energy change for reaction (1) is only slightly negative as compared to the Gibbs energy changes accompanying the formation of CO_2 and CO at the same temperature, *viz.* ΔG° (CO_2, 1073 K) = −396.09 kJ and ΔG° (CO, 1073 K) = −206.38 kJ, respectively. Theoretically, the main anode product should be elemental sulphur along with some CS_2 provided the oxygen partial pressure prevailing is very low. This will be in the vapour form at the experimental temperatures and is likely to condense along the tube or can be collected in a condenser. It is to be noted that CS_2 would be condensed in the liquid form (b.p. 46.5 °C of CS_2), leading to near-zero sulphur emission.

2.2. Materials and procedures

$CaCl_2$ and NaCl powders (Anhydrous, E. Merck, Darmstadt, Germany, >99%) were kept in an oven at 110 °C before use. The salts were weighed and mixed evenly in the molar ratio of 1:1. The salt mixture was filled in an alumina crucible (40 mm OD, 36 mm ID, 60 mm height, supplied by KERANOVA AB, Sweden), which was dried in an oven at 110 °C before use. Cu_2S powder (Alfa Aesar, 99.5%), was pressed into pellets with a diameter 16 mm and weight of ∼3 g at a pressure around 6 MPa, the pellets were sintered in argon gas (ICP 5.0, AGA gas AB, Sweden) at 400 °C for 2 h. Similar procedure was used for mixed powder (1:2 mole ratio) of Cu_2S and FeS (Alfa Aesar, tech.) to form the Cu_2S/FeS pellet. A thin copper wire, ∼0.2 mm diameter, was used to wrap the pellet. All pellets were stored in a desiccator, before attaching to an iron rod, 5 mm diameter, as the cathode. Graphite rod (4 mm diameter, LORRAINE PARIS) was used as anode. The DC power supply (hp Hewlett 6632A) was employed. Argon gas was used as the protective gas.

The crucible was filled with $CaCl_2$–NaCl salt mixture and placed in an alumina reaction tube. The reaction tube was sealed with silicone rubber stoppers. A thermocouple was positioned inside the reaction tube in contact with the bottom of the alumina crucible. The entire assembly was heated by a programmed heating pattern (EUROTHERM temperature controller) under the protection of argon gas. First, the reactor was slowly heated to 300 °C at a heating rate 2 °C/min, held for 2 h to further remove any moisture trace left in the system. The furnace was then heated at a rate of 6 °C/min to the targeted temperature. The salts were kept at this temperature for 0.5–1 h in order to ensure homogeneity of the molten salts. The electrodes were then inserted into the salt bath. Since the theoretical decomposition voltages of Cu_2O and FeS are 0.469 V and 0.467 V, respectively, while the value for Cu_2S is 0.529 V. Thus, we chosen 0.5 V in order to electrolyze possible Cu_2O and FeS without electrolyzing Cu_2S. Of course, the pre-electrolysis parameters should be improved after more electrochemical measurements have been done. After it, the electrolysis process was carried out at a predetermined cell voltage. The current change during electrolysis was recorded.

After the electrolysis, the electrodes were held above the molten salts and cooled to room temperature under argon gas protection. The cathode was washed with distilled water and subjected to an ultrasonic treatment. For Cu_2S/FeS pellet, ethanol was used for washing and subsequent ultrasonic treatment. The electrolysis pellet was then dried at 60–110 °C quickly and stored in a desiccator. The electrolysis Cu_2S/FeS pellets were subjected to analysis quickly to reduce possible oxidation of iron. The samples were analyzed by X-Ray Diffraction technique (Siemens D5000), and Scanning Electron Microscope (SEM) (JSM-840, JEOL) equipped with Energy-Dispersive X-ray Spectrometry analysis (EDS link, Oxford).

3. Results and discussion

Fig. 1a shows the XRD patterns of reduced Cu_2S pellet. It is seen that the XRD peaks show the presence of elemental Cu as well as CaS. It is also seen that the CaS content decreases with the increase of electrolysis time. The similarity in the XRD patterns for the electrolysis corresponding to 10, 12 and 20 h indicates that pure copper could be obtained after 10–12 h electrolysis at 2.2–2.8 V.

During every experimental run, a yellow powder deposit could always be observed along the tube, gas path and in the condenser without any liquid condensate indicating that the formation of CS_2 was insignificant. The yellowish powder in the condenser was confirmed to be elemental sulphur after filtration in distilled water (Fig. 1b). Since sulphur can condense in the low temperature zone of the tube and gas channels, it is difficult to collect all the sulphur in the present laboratory investigations in order to quantify this conclusion.

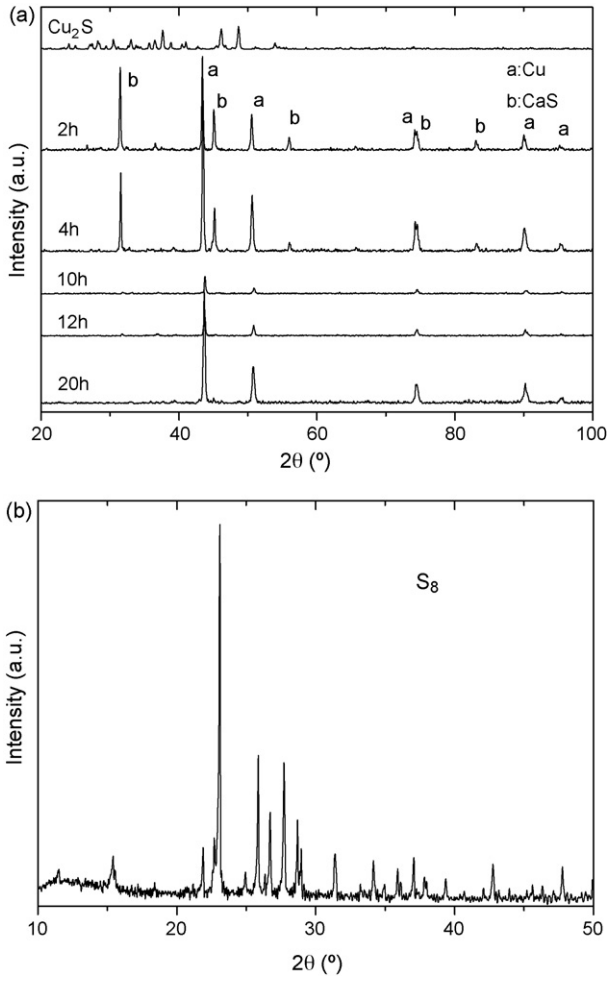

Fig. 1. X-ray diffraction patterns for electro-reduction of Cu_2S pellets at 2.8 V in molten $CaCl_2$–NaCl at 800 °C: (a) cathode products under different electrolysis time, and (b) anode product collected in the condenser after washing in distilled water.

For the electrolysis of Cu_2S, if S^{2-}/S_2 can be regarded as the reference potential, the electrode reactions of Cu_2S at 1073 K can be represented as

$$\text{anode}: S^{2-} - 2e = 1/2S_2(g), \qquad E(S^{2-}|S_2) = 0\,V \tag{3}$$

$$\text{cathode}: Cu^{+} + e = Cu, \qquad E(Cu^{+}|Cu) = -0.529\,V \tag{4}$$

Thus, when the electrolysis starts, sulphur in Cu_2S cathode gets ionized and is transported to the anode, which may cause the precipitation of CaS. In the research about the reduction of Cr_2O_3, Chen et al. [25] proposed two possible mechanisms and concluded that the calcium chromites was more likely to be formed by a chemical precipitation step. Similarly, in case of Cu_2S, the calcium sulfide precipitation can be represented as follows:

$$Cu_2S + 2e = 2Cu + S^{2-}$$

$$\text{(at the interface of electrolyte-metal-sulfide)} \tag{5}$$

$$S^{2-} + Ca^{2+} = CaS(\text{in the electrolyte}) \tag{6}$$

This would explain the presence of CaS in the cathode product in the early stages of electrolysis.

However, under a relative high voltage of 2.8 V (namely, $E(\text{vs}S^{2-}|S_2) = -2.8\,V$), the decomposition of CaS, namely, deposition of calcium also can happen:

$$\text{at 1073 K}: Ca^{2+} + 2e = Ca, \qquad E(Ca^{2+}|Ca) = -2.24\,V \tag{7}$$

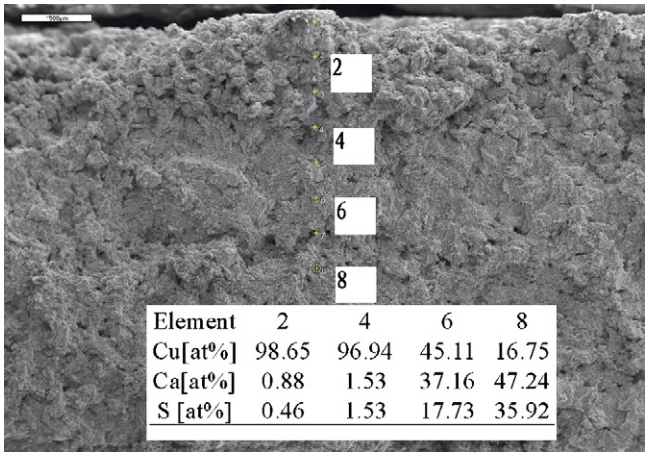

Fig. 2. Cross-section of the reduced Cu_2S pellet after 6 h electrolysis at 2.8 V in molten $CaCl_2$–NaCl at 800 °C.

which, in turn would reduce Cu_2S to Cu according to the reaction:

$$Ca + Cu_2S = CaS + 2Cu \qquad \Delta G^{\circ}(1073\,K) = -331.396\,kJ \tag{8}$$

Reaction (8) would enable the re-formation of CaS. Thus, in this case, CaS can be considered to function as a catalyst in the cathodic reaction.

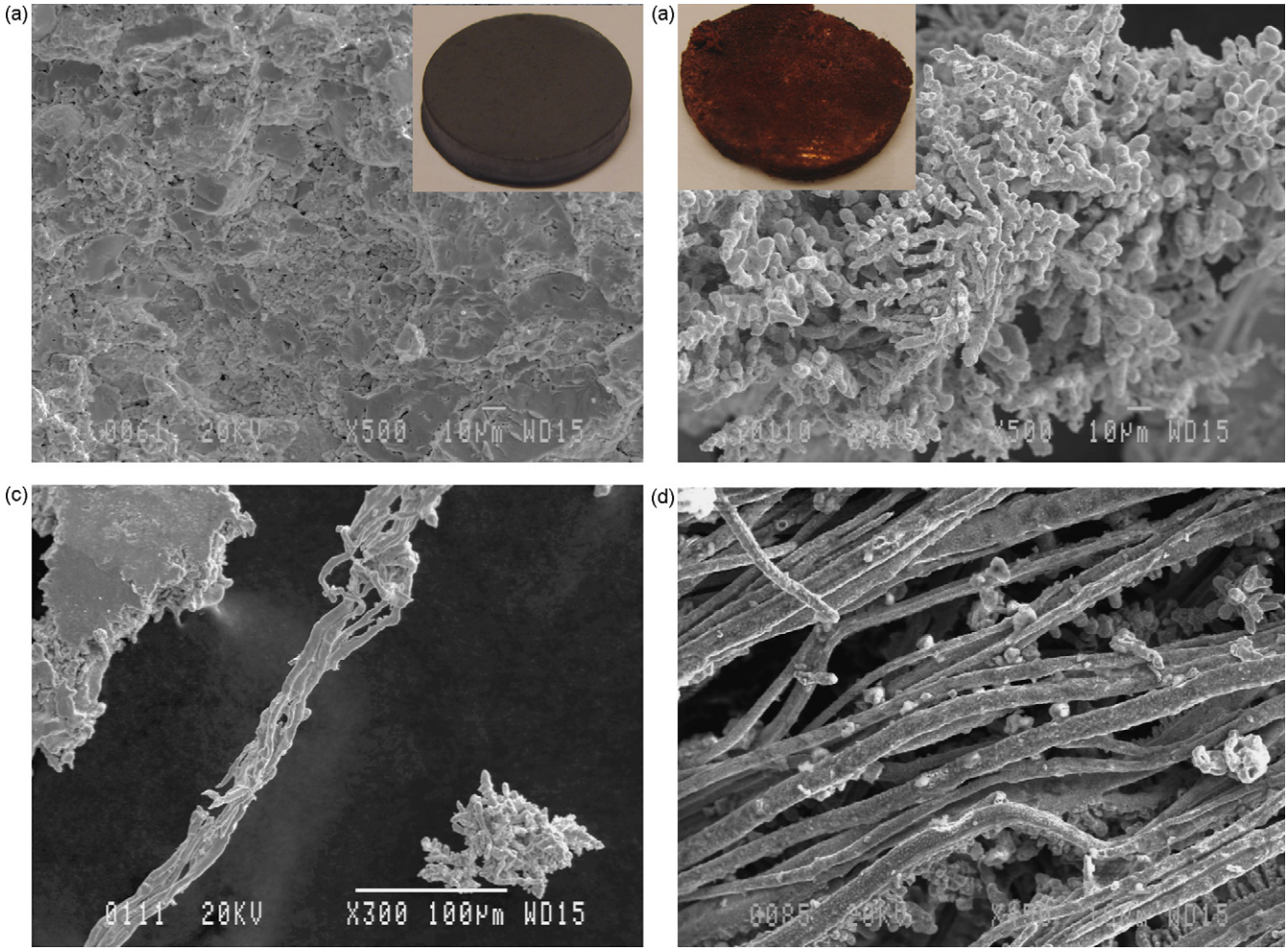

Fig. 3. Scanning electron microscopy of reduced Cu_2S pellets: (a) the surface of pellet before electrolysis, (b) Cu powder after 20 h electrolysis at 2.2 V in molten $CaCl_2$–NaCl, (c) three structures found on the outside layer, and (d) the tube structure.

If the CaS formed had a low solubility in the salt melt, it could be present in the form of Ca^{2+} and S^{2-}. As electrolysis proceeds further, CaS will dissociate into Ca^{2+} and S^{2-}. The S^{2-} ions would be transported to the anode during the electrolysis and would be oxidized at the anode to form elemental sulphur according to the anodic reaction (3).

During the present series of experiments, the graphite anode almost remained intact after every experimental run, confirming the negligible formation of the anodic product, CS_2.

EDS analysis of the different locations in a partially reduced pellet as shown in Fig. 2, indicates that the reduction pathway proceeds from outside of the pellet to the inside. Content of copper decreases towards the interior of the pellet, while Ca and S contents increase. It should be pointed out that the sample is very clean and the amount of salt, such as Na, Cl, was insignificant, even though the porous structure is probably to be filled with molten salts during electrolysis. It is admitted that the high solubility of $CaCl_2$ and NaCl in distilled water may contribute to some extent. However, it also indicates that wetting could be poor between the reduced porous copper and salt melts. This phenomenon means that the separation of copper and molten salts is quite easy.

Fig. 3 shows the SEM images of Cu_2S pellets before and after electrolysis. Fig. 3a shows the surface image of sintered pellet before electrolysis. It is seen the surface of the sintered Cu_2S pellet consists of particles with sizes varying in a wide range. After 20 h electrolysis, the pellet presents a clear appearance of copper (inset of Fig. 3b). The particles are of ~10 μm, and well sintered, showing a more complicated nodular structure. This can probably be attributed to the relatively low melting point of copper (1083 °C) and long electrolysis time of 20 h. It should be noted that Fig. 3b is taken from the inner section of the reduced pellet. This shows mainly the existence of nodular structure. Fig. 3c shows the structures corresponding to the outer part of the pellet. Here, it can be seen that, besides the nodular structure, two other interesting structures, dendritic as well as needle crystals, can be found. Fig. 3d presents a clear view of the needle structure. The typical dendritic structure shown in Fig. 3c is more likely to be formed by electrodeposition from the salt, not from the reduction of Cu_2S.

In the present experiments, no special steps were taken to purify the salt mixtures such as purification by chlorine gas. Further, high purity argon gas was used in the electrolysis experiments as supplied without taking extra precautions for the removal of traces of oxygen, moisture and carbon dioxide. This would mean that the following possible side reactions might occur:

$$Cu_2S + 1.5O_2 = Cu_2O + SO_2, \qquad \Delta G^\circ(1073\,K) = -272.09\,kJ \quad (9)$$

$$Cu_2S + O_2 = 2Cu + SO_2, \qquad \Delta G^\circ(1073\,K) = -181.55\,kJ \quad (10)$$

$$2Cu + 0.5O_2 = Cu_2O, \qquad \Delta G^\circ(1073\,K) = -90.55\,kJ \quad (11)$$

Even assuming that the partial pressure of SO_2 as 1 atm, the equilibrium oxygen pressures of the above reactions are around 1.5×10^{-9} atm, which means the above equations are highly possible.

Since $CaCl_2$ is very sensitive to the moisture, HCl gas may be generated by the reaction:

$$CaCl_2\,(salt) + 2H_2O\,(gas) = Ca(OH)_2\,(solid) + 2HCl\,(salt) \quad (12)$$

The generated HCl can react with Cu_2O according to the reaction:

$$Cu_2O + 2HCl = 2CuCl + H_2O, \qquad \Delta G^\circ\,(1073\,K) = -76.89\,kJ \quad (13)$$

CuCl has a low decomposition voltage of E_d(1073 K, CuCl) = 0.939 V, Cu can be deposited to form the dendritic crystals on the surface. Another possibility is that Cu_2S may dissolve in the salt melt to form Cu^+ and S^{2-}, and then Cu^+ gets deposited on the surface. This would explain the observation in Fig. 3c.

In the present work, an attempt was also made to explain the formation of the needle-like structure close to the surface as shown in Fig. 3c and d. For the needle structure, further investigations show that these are actually tubes in micrometer size, the formation of which can also be attributed to the electrochemical deposition. It is known from earlier work [26–28] that Cu nanotube can be synthesized by the direct electrochemical deposition on a porous membrane with very careful treatment to obtain the ideal orientation. Nanotubes without very good orientation even can grow from a copper coil without any template and additives [29]. Under the present experimental conditions, the number of pores on the outer layer of the pellet is significant as can be seen in Fig. 3a. With the removal of sulphur during the electrolysis, the porosity would increase. The likelihood of copper getting deposited along the pores to form a tube would be high, in analogy with a porous membrane. Consequently, micrometer size pores close to the surface of the pellet would lead to the formation of the tube structure in the micrometer size (Fig. 3d). However, preliminary experiments suggest that these two structures, which are confined to the outer layer can, to a smaller extent, be controlled by a stringent control of the chemistry of the salt mixture and the purity of the gas atmosphere as further sulphur depletion from the surface can occur leading to higher porosity.

The current efficiency and energy consumption can be estimated from the current–time plots during electrolysis in combination with corresponding sulphur contents in the electrolysis products by chemical analysis. In the case of pure Cu_2S, shown in Fig. 4a,

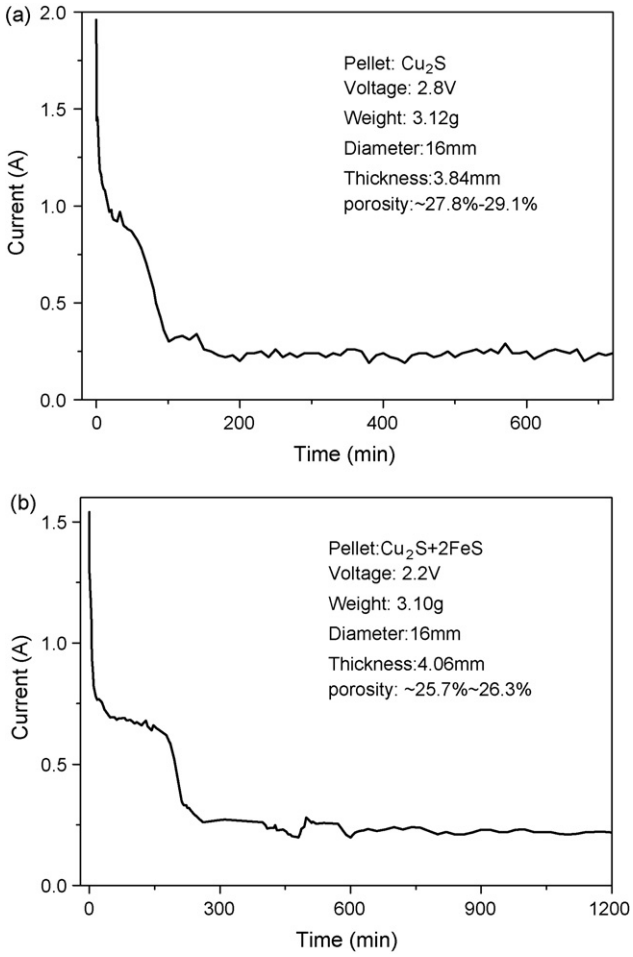

Fig. 4. Typical current–time plots for pellet reduction in molten $CaCl_2$–NaCl at 800 °C. Pellets are sintered at 400 °C in argon: (a) Cu_2S pellet, and (b) Cu_2S/FeS pellet.

the current shows a sudden drop within the first 20 min. After a short delay, the decrease in current continues and reaches a steady value after 1–2 h lasting until the termination of electrolysis. The current efficiency estimated from Fig. 4a is 32.8%, corresponding to 3.60 kWh/kg Cu. However, the current efficiency is not very high and actually it is also a major obstacle in reduction of many oxides. The current efficiency depends on a number of factors such as pellet thickness and porosity, etc. Under similar conditions, thicker and denser pellets showed a lower current efficiency. Strict control of electrolysis procedures and conditions are also important. More importantly, since reduction of Ca^{2+} to a low valence state, e.g. Ca(0) and Ca(I) is highly likely to occur, this will not only lower the current efficiency as a side-reaction, but also increase the electronic conductivity of the molten salt, which can bring about a relative high background current [5]. Further, the removal of the last amount of S^{2-} is a slow process in comparison with the reduction of Cu_2S phase. Thus, current efficiency is significantly influenced by the background current. When electrolyzed at 2.8 V, the current efficiency is estimated to be 74.08% for 2 h electrolysis, 46.61% for 4 h and 16.56% for 20 h. Probably, in order to improve the current efficiency, the low porosity (~28%) in the present experiment can be increased by employing a lower pressure (below 6 MPa) in pressing the pellets or having additives, which would evaporate leaving cavities. However, great effort is still necessary to reduce or eliminate the background current.

Attempts were also made in the present investigation to study the electro-reduction of chalcopyrite. But the chalcopyrite pellet started disintegrating during the process, leading inevitably to material loss into the bulk electrolyte. Preliminary experiments with chalcopyrite show that prior heating of $CuFeS_2$ in argon was essential, during which part of sulphur may be lost. The matte remaining could then be pressed to form the porous pellet and subjected to electro-reduction. A selective leaching step by hydrometallurgy in order to separate Cu and Fe is being currently developed and the results are expected to be reported shortly. In the present work, Cu_2S and FeS mixed powder (1:2 mole ratio) was employed to avoid this problem. A similar change of current was observed in the case of compacts of a mixture of Cu_2S and FeS pellets as can be seen in Fig. 4b. The current efficiency for the electro-reduction of Cu_2S/FeS compacts was estimated from Fig. 4b to be 23.76%, with an energy consumption of 6.23 kWh/kg (CuFe).

XRD patterns of the reduced Cu_2S/FeS pellets are presented in Fig. 5a. One can see that iron is reduced first, probably due to a lower decomposition voltage of E_d(1073 K, FeS) = 0.467 V. Even in this case, CaS was found in the XRD patterns indicating the formation of the same as an intermediate product. The amount of CaS was found to be decreasing with the increase of electrolysis time and after 20 h electrolysis, it was totally absent. The product consisted only of copper and iron. EDS analysis shows that the electrolysis product, in fact, was a two-phase mixture of copper and iron, which would be in accordance with Cu–Fe phase diagram. Fig. 5b shows a Cu-rich particle surrounded by the CaS particles in a partially reduced pellet.

The results obtained so far show a promising green process route for treatment of copper ore by the electro-reduction method. However, further work is needed to be carried out in order to understand the reduction mechanism of pellet, formation of the dendritic- and needle-structure, collection of anode sulphur, optimization of process parameters such as cell voltage, sintering temperature and pellet porosity to improve the current efficiency, etc.

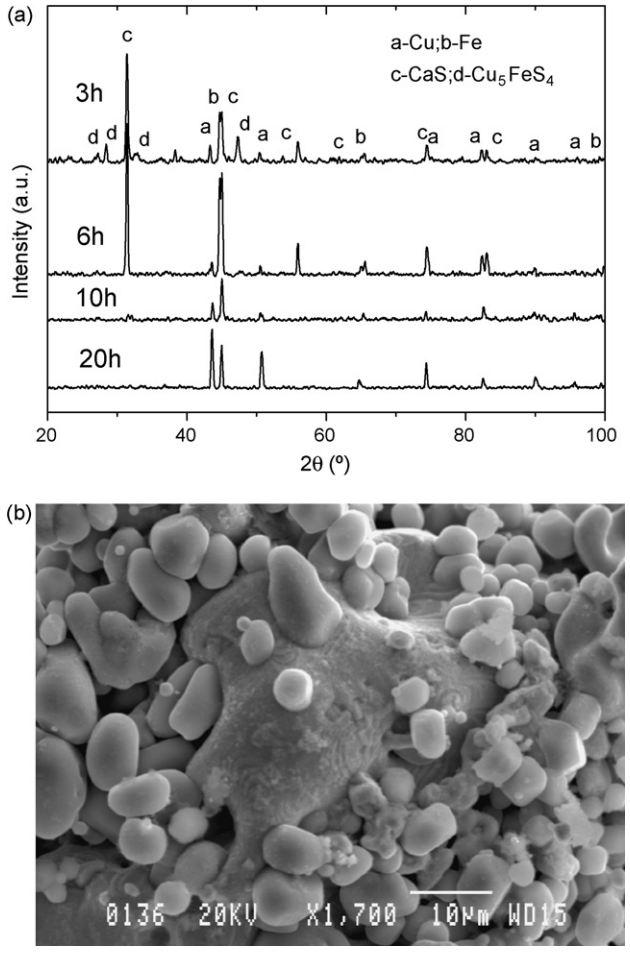

Fig. 5. Treatment of Cu_2S/FeS: (a) XRD patterns of reduced Cu_2S/FeS pellet at 2.8 V in molten $CaCl_2$–NaCl at 800 °C, and (b) SEM image of a Cu-rich particle in a partially reduced Cu_2S/FeS pellet.

4. Conclusions

In the present work, a potential process for copper extraction from copper ores in molten $CaCl_2$–NaCl melts is put forward by an electro-reduction method without SO_2 emission. The sintered solid porous Cu_2S or Cu_2S/FeS pellets can be electrolyzed to elemental Cu, S and Cu, Fe, S under a cell voltage 2.2–2.8 V at 800 °C by the evidence of XRD patterns. CaS can be formed as the intermediate product in the early stage of electrolysis. SEM/EDS results prove that the reduction proceeds from outside to inside of the pellets. The particles are well sintered, and a small amount of deposits with dendritic- and needle-like structures were found at the outside layer of the reduced pellets. The formation of these structures is attributed to the electrodeposition of copper due to the side-reactions. However, the electro-reduction process is less sensitive to factors that can cause side reactions and thus, is suitable for industrial applications. The current efficiency estimated for Cu_2S pellets is 32.8%, corresponding to 3.60 kWh/kg Cu; and 23.76%, with an energy consumption of 6.23 kWh/kg (CuFe) for reduction of Cu_2S/FeS compacts. All the results presented here show a promising green process route for treatment of copper ore by this electro-reduction method.

Acknowledgements

The Swedish Foundation for Strategic Environmental Research (Mistra, project No. 88032) and Natural Science Foundation of China (No. 50425415) are acknowledged for the financial support of this work. The first author is grateful to the content of the analysis for anode product from Li et al. [21].

References

[1] A.K. Biswas, W.G. Davenport, Extractive Metallurgy of Copper, Pergamon, 2002.
[2] G.Z. Chen, D.J. Fray, T.W. Farthing, Nature 407 (2000) 361.
[3] D.J. Fray, G.Z. Chen, Mater. Sci. Technol. 20 (2004) 295.
[4] D.H. Wang, X.B. Jin, G.Z. Chen, Annu. Rep. Prog. Chem. C 104 (2008) 189.
[5] M. Ma, D.H. Wang, W.G. Wang, X.H. Hu, X.B. Jin, G.Z. Chen, J. Alloys Compd. 420 (2006) 37.
[6] K. Pritish, W.E. James, Electrochim. Commun. 8 (2006) 1397.
[7] C. Schwandt, D.J. Fray, Electrochim. Acta 51 (2005) 66.
[8] K. Dring, R. Dashwood, D. Inman, J. Electrochem. Soc. 152 (2005) E104.
[9] K. Dring, R. Dashwood, D. Inman, J. Electrochem. Soc. 152 (2005) D184.
[10] X.B. Jin, P. Gao, D.H. Wang, X.H. Hu, G.Z. Chen, Angew. Chem. Int. Ed. 43 (2004) 733.
[11] D.T.L. Alexander, C. Schwandt, D.J. Fray, Acta Mater. 54 (2006) 2933.
[12] T. Nohira, K. Yasuda, Y. Ito, Nat. Mater. 2 (2003) 397.
[13] X.Y. Yan, D.J. Fray, Adv. Funct. Mater. 15 (2005) 1757.
[14] K. Yasuda, T. Nohira, Y. Ito, J. Phys. Chem. Solids 66 (2005) 443.
[15] K. Yasuda, T. Nohira, R. Hagiwara, Y.H. Ogata, Electrochim. Acta 53 (2007) 106.
[16] Y. Sakamura, M. Kurata, T. Inoue, J. Electrochem. Soc. 153 (2006) D31.
[17] A.M. Abdelkader, A. Daher, R.A. Abdelkareem, E. El-Kashif, Metall. Mater. Trans. B 38B (2007) 35.
[18] K. Dring, R. Bhagat, M. Jackson, R. Dashwood, D. Inman, J. Alloys Compd. 419 (2006) 103.
[19] R. Bhagat, M. Jackson, D. Inman, R. Dashhood, J. Electrochem. Soc. 155 (2008) E63.
[20] M. Kurata, T. Inoue, J. Serp, M. Ougier, J.P. Glatz, J. Nucl. Mater. 328 (2004) 97.
[21] G.M. Li, D.H. Wang, X.B. Jin, G.Z. Chen, Electrochem. Commun. 9 (2007) 1951.
[22] G.Z. Chen, D.J. Fray, J. Appl. Electrochem. 31 (2001) 155.
[23] FactSage 5.5. CRCT-ThermFact and GTT-Technologies, 2006.
[24] C.W. Bale, P. Chartrand, S.A. Degterov, G. Eriksson, K. Hack, R. Ben Mahfoud, J. Melançon, A.D. Pelton, S. Petersen, Calphad 26 (2002) 189.
[25] G.Z. Chen, E. Gordo, D.J. Fray, Metall. Mater. Trans. B 35B (2004) 223.
[26] Y.H. Wang, C.H. Ye, X.S. Fang, L.D. Zhang, Chem. Lett. 33 (2004) 166.
[27] D.C. Yang, G.W. Meng, S.Y. Zhang, Y.F. Hao, X.H. An, Q. Wei, Y. Min, L.D. Zhang, Chem. Commun. (2007) 1733.
[28] D.M. Davis, E.J. Podlaha, Electrochem. Solid State Lett. 8 (2005) D1.
[29] X.F. Wu, H. Bai, J.X. Zhang, F.E. Chen, G.Q. Shi, J. Phys. Chem. B 109 (2005) 22836.